



# Influence of temperature on corrosion behavior of PbCaSnCe alloy in 4.5 M H<sub>2</sub>SO<sub>4</sub> solution

Yan Mi-Lin\*, Zhao Wen-Zhen

School of Materials Science and Engineering, Xi'an Jiaotong University, Xi'an 710049, China

## ARTICLE INFO

### Article history:

Received 1 May 2009

Received in revised form 1 July 2009

Accepted 8 July 2009

Available online 23 July 2009

### Keywords:

Potentiodynamic curve

Electrochemical impedance spectra (EIS)

Mott–Schottky plot

Photocurrent response

PbCaSnCe alloy

## ABSTRACT

The temperature effect on corrosion behaviors of PbCaSnCe alloy in 4.5 M H<sub>2</sub>SO<sub>4</sub> solution was investigated by using potentiodynamic curve, electrochemical impedance spectra (EIS), Mott–Schottky plot and photocurrent response methods. It was found that PbCaSnCe alloy was in passive state in sulfuric acid solution, a passive film can be formed on alloy surface. The compositions of passive films formed at 0.9 V for 2 h under different temperatures were detected by X-ray photoelectron spectroscopy (XPS). The results showed that the film resistance and the transfer resistance decreased with the increment of the solution temperature. Mott–Schottky analysis and the photocurrent response revealed that the passive film exhibited n-type semi-conductive character, the donor density of the passive film decreased with increasing the solution temperature. Photocurrent response revealed that the photocurrent increased with increasing temperature. XPS results indicated that the PbO<sub>2</sub> content in passive films may increase with increasing the solution temperature.

© 2009 Elsevier B.V. All rights reserved.

## 1. Introduction

Generally, passive films formed on metals or alloys play an important role in protecting metals or alloys from further corrosion, the protective nature of passive films is supposed to be connected with their electronic properties. Many researches have been performed on this problem [1–4]. Passive films formed on lead or lead alloys in sulfuric acid solution, are different to other passive films considering the factual operation condition of lead or lead alloys in lead acid battery, passive films on lead or lead alloys should have the following two characteristics: firstly, passive films should have good protection on the substrate; secondly, passive films should also have good electronic conductive property, because passive films exist between the active material and substrate, better electronic conductive property of passive films better charging–discharging performance of lead acid battery is.

PbCa and PbSb alloys are widely used as grid materials in lead acid battery [5,6]. However, two alloys have their demerits. For PbSb alloy, it may accelerate the gas evolution and self-discharge phenomena for lead acid battery, and then may make the battery capacity loss prematurely [7–9]. For PbCa alloy, a serious problem is now usually referred to as premature capacity loss (PCL), it is related to an high impedance passive film easily formed between the positive grid and the active material, the dominant composition

of this layer is PbO, which has an undesirable effect of increasing the impedance of the anode after storage for a certain period of time, then, the premature capacity of lead acid battery decreased sharply [10–13]. To better resolve the PCL problem, Ce was added into PbCaSn alloy, according to Li and Liu [14–16], Ce can effectively decrease the resistance of the anodic film on PbCaSn alloy, and therefore it can improve the deep recycle performance.

It is well known that lead acid battery may be suffered from temperature changing during the factual operation; the temperature changing may affect the corrosion property of PbCaSnCe alloy in sulfuric acid solution, and then it may affect the battery operation performance. While, there are fewer papers focused on this issue according to the published papers.

The objective of this work is to determine the influence of temperature on the electronic property of the passive film on PbCaSnCe alloy by potentiodynamic curve, electrochemical impedance spectroscopy (EIS), Mott–Schottky analysis and photocurrent response.

## 2. Experimental

### 2.1. Sample preparation

The sample was prepared by melting weighed mixtures of pure lead (99.99 wt.%), pure tin (99.99 wt.%), pure calcium (99.99 wt.%) and pure cerium (99.99 wt.%) with a crucible in an electric furnace, nitrogen gas was pulled on the molten surface to protect the oxidation of Ca, Sn and Ce, the molten metal flowed from the bottom of the furnace. The molten lead was poured into a copper mould

\* Corresponding author. Tel.: +86 29 82668614; fax: +86 29 82663453.  
E-mail address: [ymltgrc@126.com](mailto:ymltgrc@126.com) (Y. Mi-Lin).

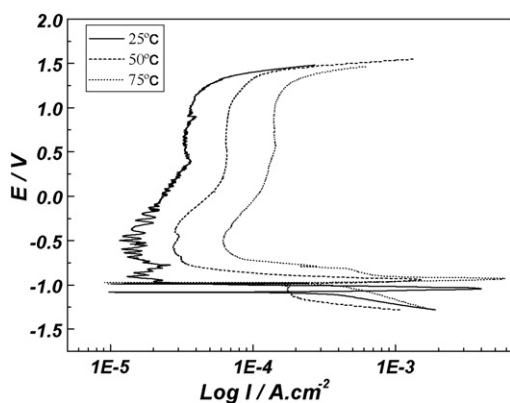


Fig. 1. The potentiodynamic curves of PbCaSnCe alloy in 4.5 M H<sub>2</sub>SO<sub>4</sub> solution at different temperatures.

of 500 K in the atmosphere to form the rod ( $\Phi 20$  mm  $\times$  200 mm) sample. The compositions of the casting alloys were determined by chemical analysis and the results were listed as following: 0.045 wt.%Ca, 1.35 wt.%Sn, 0.05 wt.%Al, 0.05 wt.%Ce and Pb balance. The rod samples were manufactured in a form of wafer ( $\Phi 5$  mm  $\times$  5 mm), one of the end surface was exposed in the electrolyte acting as the working surface polished with emery paper of successively decreasing grain size down to about 10  $\mu$ m, others were sealed with epoxy resin in the lower part of an L-shaped glass tube. Then, the working electrode was washed with double-distilled water before being immersed in the electrolyte. The electrolyte was 4.5 mol/L H<sub>2</sub>SO<sub>4</sub> solution prepared from A.R. H<sub>2</sub>SO<sub>4</sub> and double-distilled water.

## 2.2. Electrochemical experiments

A conventional three-electrode electrochemical cell was used, the counter electrode was a Pt wire, and all potentials were measured against an Hg/Hg<sub>2</sub>SO<sub>4</sub> electrode. All the electrochemical experiments were performed at EG&G Model 273 potentiostat/galvanostat with M5210 lock-in amplifier. Before experiment, a cathodic polarization at a potential of  $-0.6$  V (vs. OCP) for 20 min was carried out in order to remove any oxidation products formed by aerial.

For Mott–Schottky plot, the scanning potential range was from  $-0.4$  V to 1.0 V with a scanning rate of 2 mV, the measured frequency was 1000 Hz. For EIS, the potential was increased by 10 mV, the sweeping frequency was from 100 kHz to 10 mHz, and the measured potential was 0 V (vs. OCP).

The photocurrent measurement was made of a conventional three electrode cell of 1-multi neck flash with a quartz window as a photon inlet, a 300 W Xenon arc lamp was used as a light source, a monochromatic light with a wavelength from 200 nm to 800 nm was provided by a scanning digital monochromator controlled by a stepping motor at a scan rate of 5 nm/S, the applied potential was +300 mV, auxiliary focusing lenses were used to raise the intensity of photons toward the monochromator.

Surface analysis of X-ray photoelectron spectroscopy (XPS) was carried out with VEGA Scientific MKII(ESCALAB) apparatus, using Al K $\alpha$  X-ray source. The X-ray power was 40 W, Pb<sub>4f</sub>, S<sub>2p</sub>, and O<sub>1s</sub> binding energies were determined with C<sub>1s</sub> (284.60 eV) reference.

## 3. Result and discussion

### 3.1. The potentiodynamic curves

Fig. 1 showed the potentiodynamic curves of PbCaSnCe alloy in 4.5 M H<sub>2</sub>SO<sub>4</sub> solution at different temperatures. It can be seen that

PbCaSnCe alloy was in passive state within the potential region of  $-0.5$  V to 1.1 V, it was related to the formation of the passive film in this potential region. In general, passive film can act as the ion barrier existed between the substrate and the corrosion electrolyte, then it can effectively protect the substrate from further corrosion. Fig. 1 obviously showed that the steady passive current increased and the steady passive potential region decreased with increasing the solution temperature, it mean that the corrosion tendency of PbCaSnCe alloy in 4.5 M H<sub>2</sub>SO<sub>4</sub> solution increased with increasing temperature, and then, we can conclude that the protection of the passive film on PbCaSnCe alloy decreased.

### 3.2. Electrochemical impedance spectra

Electrochemical impedance spectra (EIS) has been widely used to study and characterize passive films anodically formed on pure metals or alloys [17,18], whose electronic properties are expected to be of crucial importance in understanding of their protective character. For the working electrode, it was firstly passivated at 0.4 V, 0.7 V and 0.9 V for 2 h at different temperatures to form passive films, respectively. Impedance spectra were then performed at the formation temperatures. Fig. 2(a), (b) and (c) showed that the Nyquist plots of the passive films formed at different potentials for 2 h at 25 °C, 50 °C and 75 °C, respectively. It can be noticed that the Nyquist plots displayed similar features, i.e., Nyquist plots were composed of two depressed semicircles, the low frequency semicircle was very flattened for each temperature and had the appearance of diffusion character. The semicircle decreased with increasing potential at one fixed temperature and increased with decreasing temperature at one fixed potential, it indicated that the film protection decreased with increasing temperature and potential. Several models of circuits to fit these experimental data were attempted. The best agreement between experiment and fitting were obtained with the equivalent circuit illustrated in Fig. 2(d). As showed in Fig. 2(d),  $R_s$  is the solution resistance,  $Q_1$  representing the capacitance of the double layer,  $R_1$  is related to the transfer resistance,  $Q_2$  and  $R_2$  are the capacitance and resistance of the passive film,  $Y_w$  is the parameter depicted the diffusion property, the value of  $Y_w$  is inverse to the value of diffusion coefficient  $D_0$ , respectively.

In the circuit model, a constant phase element (CPE) was used. The impedance ( $Z$ ) of a CPE can be obtained with the following relationship [19,20].

$$Z_{\text{CPE}} = [Q(jw)^n]^{-1} \quad (1)$$

where  $w$  is the frequency of alternative current,  $Q$  is the combination of properties related to both the surface and the electroactive species, and exponent  $n$  is the slope of the impedance-frequency Bode plot. CPE has the properties of a capacitance when  $0.5 < n < 1$ . The fitted results were listed in Table 1. It can be seen that the transfer resistance  $R_1$  and film resistance  $R_2$  decreased with the increment of temperature and potential, while the value of  $Y_w$  and the film capacitance  $Q_2$  increased, the values of the exponent  $n$  obtained by fitting the EIS data were between 0.68 and 1. The increment of  $Y_w$  value indicated that the ion diffusion resistance decreased, the decrement of  $R_1$  and  $R_2$  indicated that the corrosion tendency increased, the increment of  $Q_2$  showed the decreased compact property of the passive film. According to the fitted results and the above illustrations, it can be concluded that the protective effect of the passive film on the substrate decreased with the increment of temperature. The temperature effect on the EIS results can be explained as following: according to Pavlov and Iordanov [21], the electrode system Pb/PbO layer/PbSO<sub>4</sub> membrane/H<sub>2</sub>SO<sub>4</sub> solution forms when a lead electrode immersed in an H<sub>2</sub>SO<sub>4</sub> solution is in the potential range between  $-400$  mV and  $+960$  mV (vs. the Hg/HgSO<sub>4</sub> electrode), i.e., passive films formed at the experimental

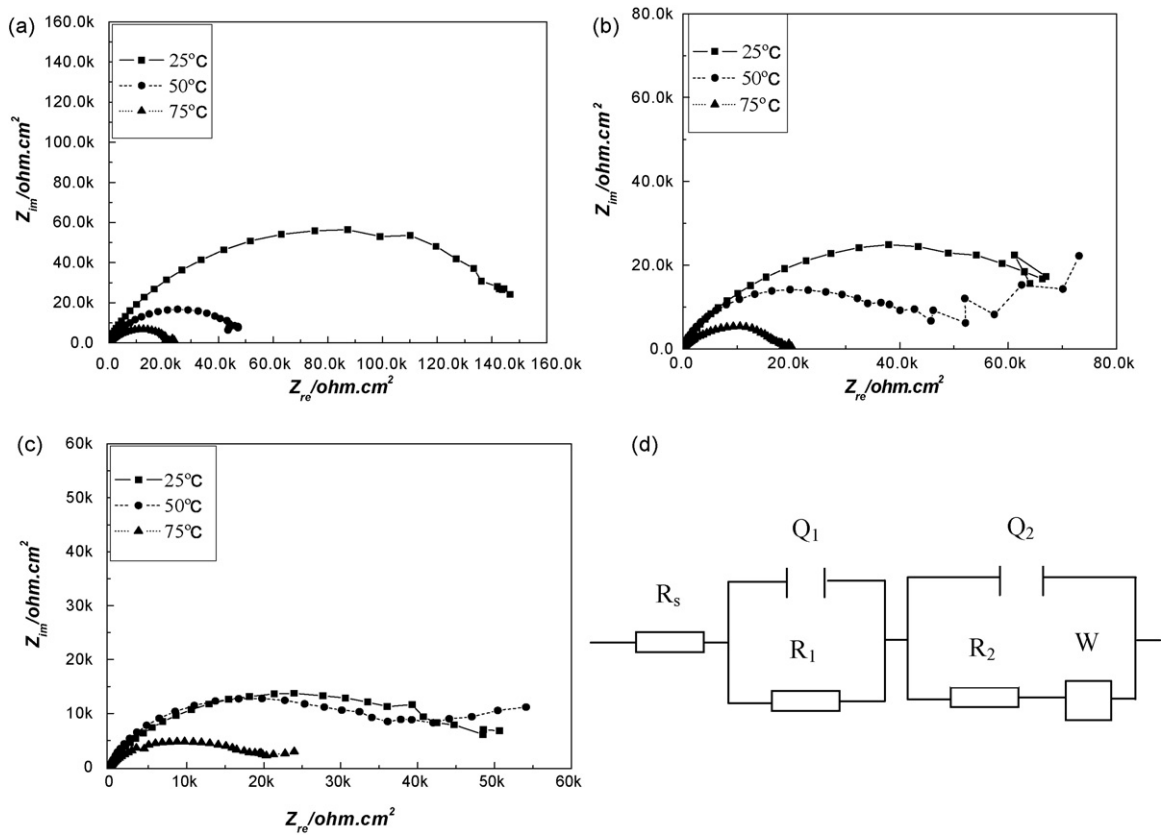


**Fig. 2.** The Nyquist plots and equivalent electron circuit of the passive films formed at different potentials for 2 h and different temperatures, (a) 0.4 V; (b) 0.7 V; (c) 0.9 V; (d) equivalent electron circuit.

potentials were mainly composed of a porous layer of  $\text{PbSO}_4$  crystals and a dense layer of t-PbO located between Pb and  $\text{PbSO}_4$  [22]. As  $\text{PbSO}_4$  is a semi-permeable membrane, in which  $\text{H}^+$  and  $\text{OH}^-$  can penetrate this membrane, while  $\text{SO}_4^{2-}$  not.  $\text{PbSO}_4$  crystals may appear various sizes, the intensity of the electric field at every point of the anodic layer will be different. The smallest distance between the lead surface and the solution may lead to the largest electric field of the intercrystalline spaces. Owing to the very complex conditions of formation of the basic sulfates the latter have probably imperfect structures, considering the stability of the anodic layer, these features of the anodic layer require ions motion taking place only through the intercrystalline spaces [21]. When the solution temperature increased, the ions motion tendency enhanced, and then the oxidation tendency of t-PbO to nonstoichiometric oxide  $\text{PbO}_n$  (where  $1 < n < 2$ ) and the oxidation tendency of  $\text{PbSO}_4$  to  $\beta\text{-PbO}_2$  may be increased [23–25]. Since  $\text{PbO}_n$  is a semiconductor and  $\text{PbO}_2$  is a conductor, while t-PbO has a level in the bandgap with an energy

of 1.9 eV. Therefore the film conductivity increased, it leads to the decrement of the film resistance and transfer resistance. Additionally, the film became more inhomogeneous with the oxidations of  $\text{PbO}/\text{PbSO}_4$  to  $\text{PbO}_n/\beta\text{-PbO}_2$ , and the compactness character of the anodic film decreased, then the film capacitance increased and the ion diffusion resistance decreased.

In order to better understand the influences of temperature and potential on the electronic properties of passive films, the variations of the steady current densities of passive films formed at 0.4 V, 0.7 V and 0.9 V and the solution temperatures were measured. Fig. 3 showed the measured results, it can be seen that the passive current density increased with increasing temperature at one fixed formation potential and decreased with decreasing potential at one fixed temperature, it indicated that the protective effect of the passive film decreased and the film conductivity increased with the increment of the temperature and potential, this result was consistent with the EIS results and potential dynamic curves.

**Table 1**  
The fitted values of components in the corresponding electron-circuit.

	Temperature								
	25 °C			50 °C			75 °C		
	0.4 V	0.8 V	0.9 V	0.4 V	0.8 V	0.9 V	0.4 V	0.8 V	0.9 V
$R_s$ ( $\Omega \text{ cm}^2$ )	1.214	1.193	1.227	1.073	1.064	1.016	0.4358	0.4132	0.5042
$Q_1$ ( $10^6 \text{ F cm}^{-2}$ )	9.024	11.7	10.76	14.16	10.39	11.73	12.26	13.93	5.328
$n_1$	0.8648	0.8941	0.8915	0.8162	0.8226	0.8257	0.7783	0.689	0.7943
$R_1$ ( $10^{-4} \Omega \text{ cm}^2$ )	12.44	3.415	0.5482	4.184	1.077	0.5448	1.745	1.698	0.4962
$Q_2$ ( $10^5 \text{ F cm}^{-2}$ )	1.055	1.077	1.745	1.177	1.897	1.309	2.145	8.839	7.861
$n_2$	0.8673	0.8938	0.8962	0.901	0.8133	0.8343	0.699	0.7055	0.7864
$R_2$ ( $10^{-4} \Omega \text{ cm}^2$ )	6.623	2.613	1.148	3.455	1.322	0.4355	0.7959	0.1463	0.2659
$Y_w$ ( $10^4 \Omega^{-1} \text{ S}^{-0.5}$ )	1.813	1.995	2.462	2.867	6.176	20.61	4.455	32.34	52.65

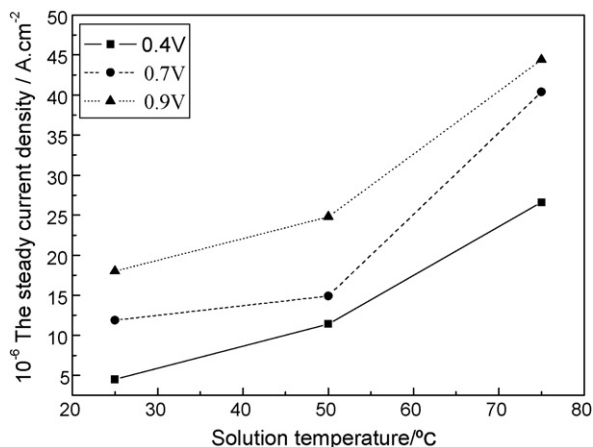


Fig. 3. The variation of steady passive current densities of the passive films formed at different potentials and the solution temperatures.

### 3.3. Mott–Schottky plot

Mott–Schottky analysis is often used to investigate the electronic property of the passive film formed on metal or alloy by measuring the electrode capacitance as a function of the potential ( $E$ ). The diffuse charge in the depletion layer of the electrode can

be conceived as a series connection of two capacitancies, is, that of the depletion layer  $C_{SC}$  and that of the Helmholtz layer  $C_H$ . Then, the potential dependence of the  $C$  of a semiconductor electrode under depletion layer can be expressed here [26,27]:

For n-type semiconductor

$$C^{-2} = C_{SC}^{-2} + C_H^{-2} + \frac{2}{C_{SC} \cdot C_H} = C_{SC}^{-2} + \frac{2}{\varepsilon \varepsilon_0 e N_D} \left( E - E_{FB} - \frac{KT}{e} \right) \quad (2)$$

where  $\varepsilon$  is the dielectric constant of the passive film,  $\varepsilon_0$  is the permittivity of the free space ( $8.854 \times 10^{-14} \text{ F cm}^{-1}$ ),  $e$  is the electron charge,  $N_D$  is the donor density,  $E_{FB}$  is the flat-band potential,  $K$  is the Boltzmann constant,  $T$  is the absolute temperature.  $KT/e$  can be negligible as it is only about 25 mV at room temperature. The values of  $C$  are obtained from Eq. (2), supposing a conservative constant value of  $20 \mu\text{F cm}^{-2}$  for  $C_H$  [28].  $N_D$  is determined from the slope of the experimental  $C^{-2}$  vs.  $E$  plots, while  $E_{FB}$  comes from the extrapolation for  $C^{-2} = 0$ .

It can be obviously seen that the slopes of the straight lines in Mott–Schottky plots appeared positive, indicating an n-type semiconductive property of passive films. The slopes of the straight lines in Fig. 4(a), (b) and (c) increased with the increment of temperature. Based on Eq. (2), it can be concluded that the donor density within the passive film decreased with increasing temperature. Assuming the dielectric constant of the passive film is 26 [29], then it can be obtained the donor densities of the passive films formed at different temperatures and at different potentials, the calculated

Table 2

The donor density of the passive films formed at different temperatures and potentials.

	Temperatures and potentials								
	25 °C			50 °C			75 °C		
	0.4 V	0.8 V	0.9 V	0.4 V	0.8 V	0.9 V	0.4 V	0.8 V	0.9 V
$N_D$ ( $10^{-19} \text{ cm}^{-3}$ )	4.679	3.423	2.943	4.574	1.531	1.5	0.566	0.483	0.318

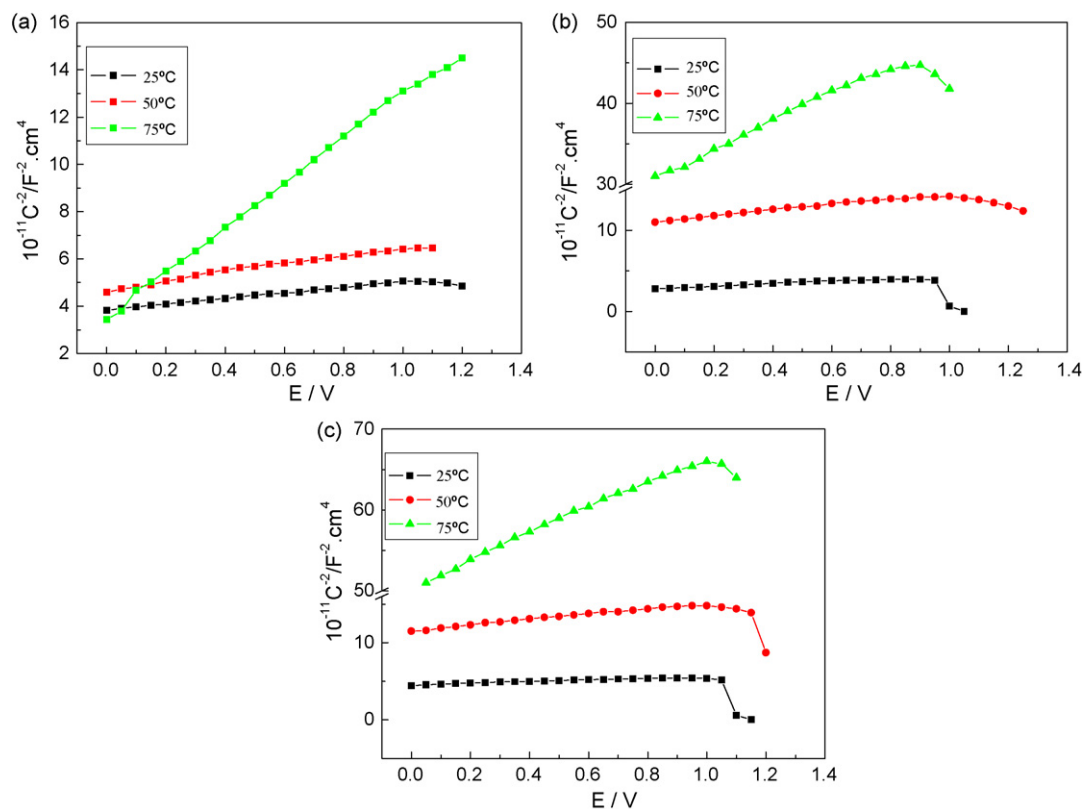


Fig. 4. Mott–Schottky plots of the passive films formed at different temperatures and different formation potentials (a) 0.4V; (b) 0.8V; (c) 0.9V.

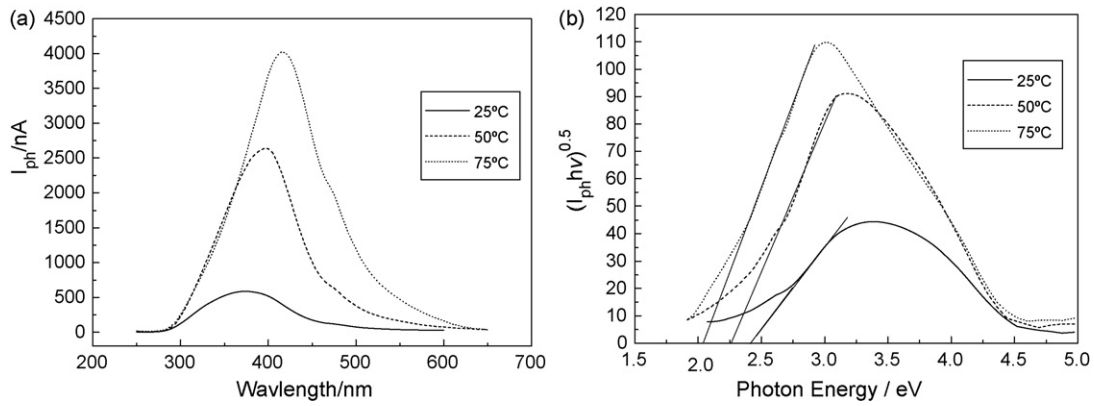


Fig. 5. The photocurrent response and  $(I_{ph} h\nu)^{0.5}$  versus incidence energy plots of the passive films formed on lead at 0.9 V in 4.5 mol/L  $H_2SO_4$  solution for 2 h at different temperatures (a), photocurrent response (b), and  $(I_{ph} h\nu)^{0.5}$  versus incidence energy plots.

results were showed in Table 2. It can be seen that the magnitude order of the donor density reached to  $10^{19} \text{ cm}^{-3}$ , the value of  $N_D$  decreased with increasing temperature and potential. The temperature effect on Mott–Schottky plots can be related to the changing of the film composition: as noted above, passive films formed at the appointed potentials were mainly composed of t-PbO and  $PbSO_4$  [21], in which t-PbO has a large bandgap energy width, while  $PbO_n$  is a semiconductor and  $PbO_2$  is a conductor. The oxidation tendency of t-PbO to  $PbO_n$  or further to  $PbO_2$  and the oxidation of  $PbSO_4$  to  $\beta$ - $PbO_2$  increased with increasing temperature and potential, then, the number of charge carrier in the anodic film decreased. Additionally, the high localized states existing in the bandgap, these localized states can also be acted as charge carrier when excitation, that is the donor or acceptor defect. The band gap width of the anodic film may decrease with increasing temperature, and then the amount the localized states will decrease, i.e., the number of the point defects decreased.

#### 3.4. Photocurrent response

Photo-electrochemical analysis is a powerful measurement widely used to examine the in situ semi-conductive properties of passive films formed on metals and alloys. The application of the photo-electrochemical technique can obtain the composition and structure of passive film. According to Jang and Park [30], the passive film formed on Ni in pH 8.5 buffer solution was composed of an inner NiO film and an outer  $Ni(OH)_2$  film using photo-electrochemical measurement. Similarly, Kim et al. [31] investigated the passive film of Cr in deaerated 8.5 buffer solution, and concluded a single or duplex layer structure depending on the film formation potential.

Fig. 5 showed the photocurrent response and  $(I_{ph} h\nu)^{0.5}$  versus incidence energy plots of the passive films formed on PbCaSnCe alloy at 0.9 V in 4.5 mol/L  $H_2SO_4$  solution for 2 h at different temperatures. Obviously, all photocurrents were positive, it indicated that passive films had an n-type semi-conductive character, the photocurrent increased with increasing temperature. Moreover, all photocurrent spectra of passive films began to increase at about 2.0 eV, for the photocurrent of the passive film formed at 25 °C, the peak photocurrent appeared at 3.37 eV; for the photocurrent of the passive film formed at 50 °C, the peak photocurrent appeared at 3.16 eV; and for the photocurrent of the passive film formed at 75 °C, the peak photocurrent reached at 2.99 eV. Evidently, the incidence energy decreased with increasing temperature, the measured results can be concluded the two points: firstly, it can be concluded that the compositions of passive films changed with the temperature variation; secondly, since the passive film is not fully

crystalline and very thin. Pavlov et al. [32] studied the photocurrent response of lead electrode in sulfuric acid solution and ascribed the response via the following four reactions assuming that the crystal lattice of PbO consists of individual molecules of PbO.

When an  $h\nu$  photon falls on a PbO “molecule” of the bulk of the PbO layer, the following photochemical reaction will take place



Which results in the creation of the pair: electron  $e^-$  - hole  $h^+$ . The electron jumps over the bandgap and passes into the conduction band of the oxide. Under the action of the electric field the holes move within the layer. However, the PbO layer contains a high concentration of structural defects, traps  $PbOd$ :



The holes interact with these traps and charged centers  $PbOd^{\cdot+}$  are formed. Such a center contains a  $Pb^{3+}$  ion. It is unstable. By taking up a second hole it transforms into a double charged center. The lead ion being of fourth valency:



The traps may also accept a photon and the next photoreaction proceeds



Since there is an electronic equilibrium between the metal and the conduction band of the  $PbO_n$  layer the increase in the electron concentration in the conduction band brought about by reactions (3) and (6) leads to an electron transfer in the metal, i.e., to the appearance of a photocurrent.

When temperature increased, t-PbO could be converted into a  $PbO_n$  layer, hence the amount of the structural defects in PbO layer increased with increasing temperature. Based on formula (4), the increased amount of  $PbOd$  traps can generate more charged centers  $PbOd^{\cdot+}$ . Subsequently, the electron number generated from formula (6) increased, and then the photocurrent increased.

The band gap  $E_g$  of the passive film has been estimated from the photocurrent spectra according to Eq. (7) on assumption of the proportional relationship between photocurrent and the optical absorption [33]:

$$I_{ph} = \frac{A(h\nu - E_g)^n}{h\nu} \quad (7)$$

where  $A$  is a constant,  $h\nu$  the photon energy, and  $E_g$  the band gap energy,  $n$  value of 2 has been used predominantly for the passive film [33]. From Eq. (7), it can be obtained that the  $(I_{ph} h\nu)^{0.5}$  is in linearity relationship with the band gap energy,  $E_g$ , then, the band gap

energy for each spectral component was determined by extrapolating the  $(I_{ph}h\nu)^{0.5}$  versus  $h\nu$  plots to the axis of photon energy. For the passive film formed at 25 °C, the linearly fitted equation was  $(I_{ph}h\nu)^{0.5} = -284.371 + 122.307E_g$ , from which the  $E_g$  was calculated to be about 2.325 eV; for the passive film formed at 50 °C, the linearly fitted equation was  $(I_{ph}h\nu)^{0.5} = -293.918 + 138.3048E_g$ , the  $E_g$  can be calculated to be about 2.125 eV; when the solution temperature reached at 75 °C, the linearly fitted equation was  $(I_{ph}h\nu)^{0.5} = -126.476 + 53.79E_g$ , the calculated  $E_g$  was 2.0185 eV. From the calculated  $E_g$  results, it can be seen that the  $E_g$  value decreased with increasing temperature. The  $E_g$  variation can be ascribed to the component changing with temperature, as illustrated above, t-PbO and PbSO<sub>4</sub> are the major components of the anodic film formed at the experimental potential, they can be converted into PbO<sub>n</sub> layer with illuminating light, the conversion tendency increased with increasing temperature. As PbO<sub>n</sub> is a semiconductor, t-PbO and PbSO<sub>4</sub> are almost insulator, therefore, the band gap energy  $E_g$  of the anodic film decreased with increasing temperature.

### 3.5. XPS results of the passive films

In order to explain the influence of temperature on the electronic behavior of the passive film formed on PbCaSnCe alloy, it is necessary to make clear the compositions of passive films at different temperatures. Fig. 6(a) is the survey X-ray photoelectron spectrum of passive films formed at different temperatures. It can be observed that the dominant elements of passive films are consistent, i.e., Pb, S, O, Sn and C elements, in which C comes from pollution through sample preparation and measurement. Fig. 6(b) is the spectrum of Pb level 4f<sub>7/2</sub> and Pb level 4f<sub>5/2</sub> in passive films, Fig. 6(c) is the spectrum of O level 1s in passive films. Table 3 lists the comparison of banding energies for compounds found in the passive film and

**Table 3**

Comparison of banding energies for compounds found in the passive film with standard data (eV).

	Compound			
	Pb <sub>4f</sub>	S <sub>2p</sub>	O <sub>1s</sub>	C <sub>1s</sub>
Standard data (eV)				
PbO <sub>2</sub>	137.40		529.00	
PbO	138.90		530.90	
PbSO <sub>4</sub>	139.40	168.60	531.20	
Experimental data (eV)				
25 °C	138.27	168.70	530.95, 529.33	284.82
50 °C	137.70	168.70	530.83, 528.95	284.70
75 °C	137.50	168.70	530.95, 528.83	284.71

their standard data, it showed that the characteristic peak binding energies of Pb<sub>4f<sub>7/2</sub></sub> in passive films formed at different temperatures are 138.27 eV, 137.70 eV and 137.50 eV, respectively; while for the characteristic peak binding energies of O<sub>1s</sub>, they are 530.95 eV, 529.33 eV, 530.83 eV, 528.95 eV, 530.95 eV and 528.83 eV, respectively. According to Veluchamy and Minoura [34] and the standard binding energy data for compounds [35], the value of the characteristic peak binding energy of Pb<sub>4f<sub>7/2</sub></sub> at three temperatures lies between the characteristic peak binding energies of PbO (138.90 eV) and PbO<sub>2</sub> (137.40 eV), and the Pb<sub>4f<sub>7/2</sub></sub> characteristic peak binding energy comes to near the characteristic peak binding energy of PbO<sub>2</sub> (137.40 eV) with increasing the solution temperature, it indicated that the anodic film can be oxidized into PbO<sub>n</sub> (1 < n < 2) at high temperature, it is consistent with the previous conclusions. Comparing the standard binding energies of O<sub>1s</sub> with the experimental ones, it can be also found that the passive film formed at high temperature is mainly composed of PbO<sub>2</sub>, the film composition can be written as non-stoichiometric compound PbO<sub>n</sub>, then, we can obtain

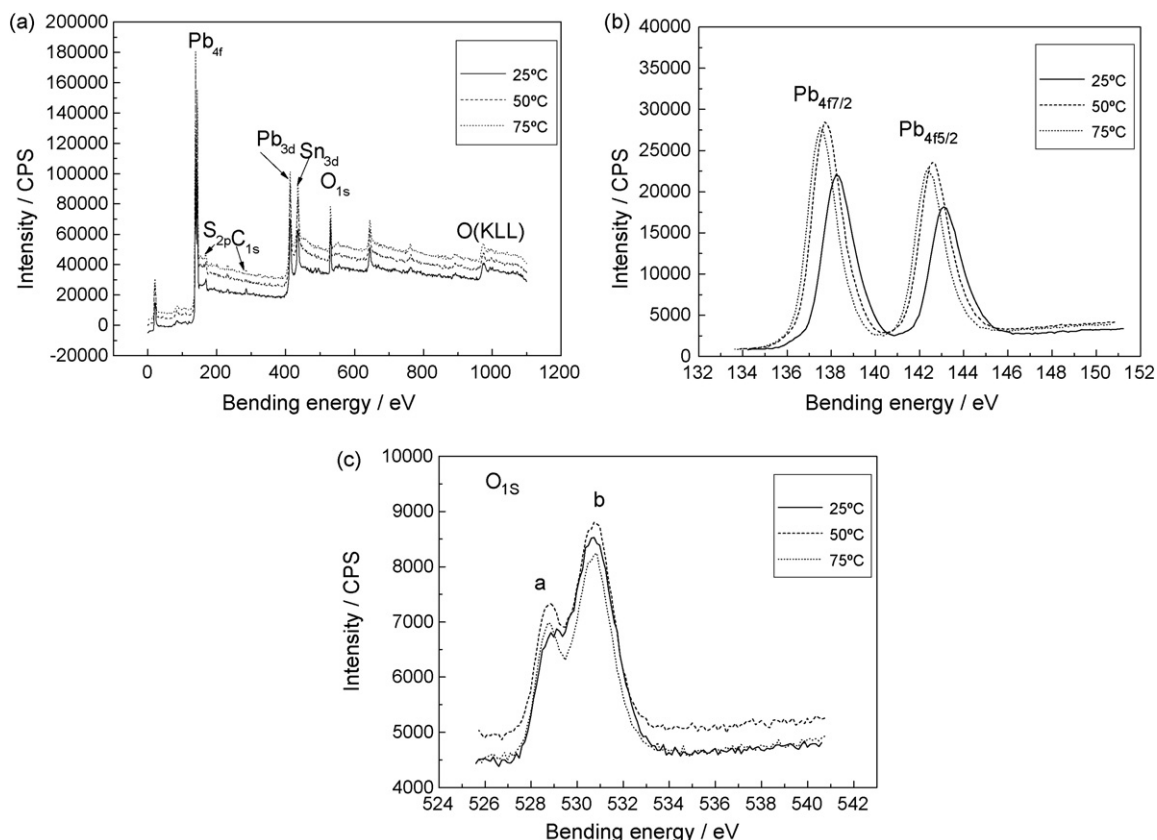


**Fig. 6.** The XPS measured results of the passive films formed at different temperatures, (a) survey spectra; (b) Pb<sub>4f</sub> character spectra; (c) O<sub>1s</sub> character spectra.

that the conductivity of the passive film enhanced with increasing the solution temperature.

#### 4. Conclusions

PbCaSnCe alloy is in the passive state in 4.5 M H<sub>2</sub>SO<sub>4</sub> solution, a passive film easily formed at the alloy surface to protect the substrate from further corrosion, the protective effect decreased with increasing the solution temperature. The passive film appears an n-type semi-conductive character, the donor density of the passive film decreased with increasing temperatures. The photocurrent response and XPS measurement results show the film conductivity increased with increasing temperature.

#### References

- [1] K. Hashimoto, K. Asami, *Corros. Sci.* 19 (1979) 251.
- [2] Q. Yang, J.L. Luo, *Electrochim. Acta* 45 (2000) 3927.
- [3] G. Okamoto, *Corros. Sci.* 13 (1973) 471.
- [4] N. Sato, K. Kudo, R. Nishimuru, *Electrochim. J. Soc.* 123 (1976) 1419.
- [5] Manahov, D. Pavlov, *J. Electrochem. Soc.* 141 (1994) 2316.
- [6] D. Pavlov, *J. Power Sources* 46 (1993) 171.
- [7] B.K. Mahato, J.L. Strebe, D.F. Wilkinson, K.R. Bullock, *J. Electrochem. Soc.* 132 (1985) 132.
- [8] R.L. Cui, S.G. Wu, *J. Power Sources* 46 (1993) 327.
- [9] T. Hirasawa, K. Sasaki, M. Taguchi, H. Kaneko, *J. Power Sources* 85 (2000) 44.
- [10] D. Pavlov, *J. Electrochem. Soc.* 136 (1989) 27.
- [11] J.L. Caillerie, L. Albert, *J. Power Sources* 67 (1997) 279.
- [12] C. Brissaud, G. Reumont, J.P. Smaha, J. Foct, *J. Power Sources* 64 (1997) 117.
- [13] A.F. Hollenkamp, *J. Power Sources* 59 (1996) 87.
- [14] D.G. Li, G.S. Zhou, J. Zhang, M.S. Zheng, *Electrochim. Acta* 52 (2007) 7787.
- [15] H.-T. Liu, J. Yang, H.-H. Liang, W.-F. Zhou, *J. Fudan Univ. (Nat. Sci.)* 38 (1999) 623.
- [16] Y.-B. Zhou, C.-X. Yang, W.-F. Zhou, H.-T. Liu, *J. Alloys Compd.* 365 (2004) 108.
- [17] E.M.A. Martini, I.L. Muller, *Corros. Sci.* 42 (2000) 443.
- [18] D. Wallinder, J. Pan, C. Lergraf, A. Delblanc-Bauer, *Corros. Sci.* 41 (1999) 275.
- [19] J. Hubrecht, M. Embrechts, W. Bogaerts, *Electrochim. Acta* 38 (1993) 1867.
- [20] K. Juttner, *Electrochim. Acta* 35 (1990) 1501.
- [21] D. Pavlov, N. Iordanov, *J. Electrochem. Soc.* 117 (1970) 1103.
- [22] D. Pavlov, *Electrochim. Acta* 13 (1968) 2051.
- [23] D. Pavlov, Z. Dinev, *J. Electrochem. Soc.* 127 (1980) 855.
- [24] D. Pavlov, *J. Electroanal. Chem.* 118 (1981) 167.
- [25] D. Pavlov, *Electrochim. Acta* 23 (1978) 845.
- [26] N. Sato, *Electrochemistry at Metal and Semiconductor Electrodes*, Elsevier, Amsterdam, 1998.
- [27] J.F. Dewald, *J. Phys. Chem. Solids* 14 (1960) 155.
- [28] W.P. Gomes, F. Cardon, *Progr. Surf. Sci.* 12 (1982) 185.
- [29] Z.-L. He, C. Pu, H.-T. Liu, W.-F. Zhou, *Acta Chim. Sin.* 50 (1992) 118.
- [30] H.-J. Jang, C.-J. Park, K. Hyuksang, *Electrochim. Acta* 50 (2005) 3503.
- [31] J.S. Kim, Eun Ae Cho, K. Hyuksang, *Electrochim. Acta* 47 (2001) 415.
- [32] D. Pavlov, S. Zanova, G. Papazov, *J. Electrochem. Soc.* 124 (1977) 1522.
- [33] U. Stimming, *Electrochim. Acta* 31 (1986) 415.
- [34] P. Veluchamy, H. Minoura, *Appl. Surf. Sci.* 126 (1998) 241.
- [35] J.E. Moulder, W.F. Stickle, P.E. Sobol, K.D. Bomben, *Handbook of X-ray Photoelectron Spectroscopy*, Chastain, 1992.